OncoTargets and Therapy

Dovepress
open access to scientific and medical research

Open Access Full Text Article

ORIGINAL RESEARCH

# Testosterone Exacerbates the Formation of Liver Cancer Induced by Environmental N-Nitrosamines Exposure: Potential Mechanisms and Implications for Human Health

Xin Yin[1], Hong-Wei Gu[2], Dan Ning[1], Yu-Sang Li[1], He-Bin Tang[1]

[1]Lab of Hepatopharmacology and Ethnopharmacology, School of Pharmaceutical Sciences, South-Central Minzu University, Wuhan, Hubei, People's Republic of China; [2]Pharmacy Department, Mental Health Center of Wuhan, Wuhan, Hubei, People's Republic of China

Correspondence: Yu-Sang Li; He-Bin Tang, Lab of Hepatopharmacology and Ethnopharmacology, School of Pharmaceutical Sciences, South-Central Minzu University, Wuhan, Hubei, People's Republic of China, Tel +0086-27-67841196; +0086-27-67842332, Email liys2006@mail.scuec.edu.cn; hbtang2006@mail.scuec.edu.cn

**Background:** Humans are frequently exposed to N-nitrosamines through various sources, including diet, cigarette smoking, contaminated water, the atmosphere, and endogenous nitrosation. Exposure to these carcinogens may also contribute to the gender-specific incidence of liver cancer, which is significantly higher in males than in females, possibly due to the influence of endogenous hormones such as testosterone. However, the effect of testosterone on N-nitrosamine-induced liver cancer and its underlying mechanism remains unclear.

**Purpose:** To investigate the effect of testosterone on the development of liver cancer induced by N-nitrosamines exposure.

**Patients and Methods:** Histopathological and immunohistochemical staining techniques were employed to analyze the expression levels and nuclear localizations of key signaling molecules, including androgen receptor (AR), β-catenin, and HMGB1, in both tumor and non-tumor regions of liver samples obtained from human patients and mice.

**Results:** The findings demonstrated a strong correlation between AR and β-catenin in the nuclear region of tumor areas. AR also showed a significant correlation with HMGB1 in the cytoplasmic region of non-tumor areas in both human and mice samples. The study further analyzed the expression levels and patterns of these three proteins during the progression of liver tumors.

**Conclusion:** This study confirms that AR has the ability to modulate the expression levels and patterns of β-catenin and HMGB1 in vivo, thereby exacerbating the progression of liver cancer induced by environmental N-nitrosamines exposure. Importantly, the effect of testosterone on the formation of liver cancer induced by environmental N-nitrosamine exposure intensifies this progression. These findings have important implications for drug safety in clinical practice and emphasize the significance of reducing N-nitrosamines exposure through conscious choices regarding diet and lifestyle to ensure environmental safety.

**Keywords:** N-nitrosamines, testosterone, exposure, hepatic carcinoma, androgen receptor

## Introduction

N-nitrosamines are a class of potent carcinogens that are widely found in the environment.[1,2] Humans can be exposed to N-nitrosamines through various sources including diet,[3,4] cigarette smoking,[1,5] contaminated water,[4,6–8] atmospheric pollution,[9,10] and endogenous nitrosation.[11,12] In the United States, it has been reported that the maximum daily exposure to N-nitrosamines is estimated to be 25,000 ± 4950 ng/d, with tobacco products (22,000 ± 4350 ng/d), food (1900 ± 380 ng/d), alcohol (1000 ± 200 ng/d), and drinking water (120 ± 24 ng/d) being the major contributors.[13] Our previous research has shown that even long-term exposure to trace amounts of N-nitrosamines at low frequencies can lead to hepatotoxicity.[14] Hepatocellular carcinoma (HCC) is the second most common cause of cancer-related deaths worldwide,[15] and the high incidence of HCC is closely associated with exposure to carcinogenic compounds such as

Received: 26 December 2023
Accepted: 11 May 2024
Published: 17 May 2024

N-nitrosamines.[16] Furthermore, epidemiological studies have suggested that gender differences play a significant role in the progression of liver diseases, including viral-induced liver injuries, hepatitis, hepatocirrhosis, and ultimately HCC.[17] It has also been observed that the morbidity of HCC shows a sex difference of over 2:1, with male cases accounting for 35.2 per 100,000 individuals compared to 13.3 per 100,000 in females.[18,19] However, the underlying reasons for this gender disparity still require further investigation.

Testosterone, an anabolic steroid, serves as the primary male sex hormone in the human body. It plays a crucial role in the development of male reproductive organs and the promotion of secondary sexual characteristics. Furthermore, it is associated with overall health and well-being for both men and women.[20] In addition to its natural occurrence, testosterone is also widely used as a medication in the form of testosterone propionate (TP) or 5-alpha-dihydrotestosterone (DHT) to address low testosterone levels in men and breast cancer in women. Moreover, several studies have investigated the effects of testosterone therapy in men with cirrhosis.[21] It is worth noting that rigorous attention must be paid to safety concerns prior to conducting any clinical trials. However, as far as our knowledge extends, it remains unclear whether commonly utilized testosterone exacerbates N-nitrosamines-induced liver cancer and its underlying mechanism. Therefore, studying the hepatotoxicity resulting from combined exposure to N-nitrosamines and testosterone, as well as elucidating the underlying mechanism, holds significant importance in guiding drug safety in clinical practice and ensuring environmental safety in specific conditions.

The androgen receptor (AR) serves as the direct downstream target of testosterone in the body.[1] Previous observations have shown elevated levels of AR in HCC tissues.[22] Further investigations have revealed a correlation between AR overexpression and the formation, metastasis, and invasion of HCC.[22–24] The AR functions as a transcriptional factor that, upon activation, dissociates from heat shock proteins (Hsp) and translocates from the cytosol into the nucleus to regulate the transcription and expression levels of downstream genes by binding to specific regions of DNA known as androgen responsive elements (ARE).[22,25–27] However, in vivo assessments of AR activation in animal models have not been thoroughly examined.

A potential downstream target of the androgen receptor (AR) is the Wnt/β-catenin signaling pathway, which can be activated through the activation of cell cycle-related kinase (CCRK).[28] Upon phosphorylation of glycogen synthase kinase-3beta (GSK-3β), β-catenin accumulates in the cytosol and translocates into the nucleus of liver cells.[29] It then binds to transcriptional activators, sequentially activating downstream cancer-related genes such as proliferation factors c-myc and cyclinD1, migration-related factor CD44, and invasion-related genes MMPs. Consequently, the expression levels and patterns of β-catenin are strongly correlated with hepatocellular carcinoma (HCC). Furthermore, mutations in β-catenin, which may lead to its malfunction, have been associated with one-third of liver cancer patients.[30] However, a detailed in vivo evaluation of the relationship between AR and β-catenin is currently lacking.

The high mobility group box 1 protein (HMGB1), expressed ubiquitously in the nucleus of almost all eukaryotic cells, interacts with nucleosomes, transcription factors, and histones to regulate DNA replication, repair, recombination, and transcription.[31] After phosphorylation and acetylation, HMGB1 is translocated into the cytosol[32] and subsequently secreted into the intercellular space as an inflammatory cytokine mediator.[33] HMGB1 has been shown to be associated with the activation of cancer-related transcription factors p53, p73, and NF-κB in the nucleus, promoting the invasion of cancer cells.[34–37] Additionally, HMGB1 can activate matrix metalloproteinase-9 (MMP-9) and −2 through the NF-κB pathway, facilitating the invasion of cancer cells.[38] Moreover, HMGB1 is capable of promoting the migration of cancer cells by inducing Ca2+ influx and subsequently stimulating the production of growth factors.[39] However, the upstream regulators of HMGB1 during the progression of liver cancer remain to be elucidated.

Therefore, the main objectives of this study were as follows: (1) To evaluate the effect of testosterone on the formation of liver cancer induced by environmental N-nitrosamines exposure. The study aimed to understand whether testosterone exacerbates the development of liver cancer in the presence of N-nitrosamines. (2) To investigate the expression levels and patterns of key signaling molecules including androgen receptor (AR), β-catenin, and HMGB1. This analysis was conducted in both mice and liver cancer samples from human patients. The study aimed to determine how these molecules are expressed and correlated in the context of liver cancer. (3) To propose an underlying mechanism for hepatotoxicity caused by combined exposure to N-nitrosamines and testosterone. The study aimed to elucidate the

molecular pathways and interactions that contribute to liver damage resulting from the simultaneous exposure to N-nitrosamines and testosterone.

# Materials and Methods

## Human Samples

Tissue samples from thirty-four HCC patients were obtained from and monitored by the depository of Key Laboratory of Chinese Internal Medicine of MOE, Beijing Dongzhimen Hospital, Beijing University of Chinese Medicine. Professional pathologists examined the malignant areas that were taken from carcinoma tissues, while the non-cancerous regions were obtained from normal tissues located more than 3cm away from the borderline of the cancerous region on the same fixed section. All patients involved in the clinical samples provided written informed consent, which was in accordance with the ethical requirements of the Helsinki Declaration. All pathological tissue samples were collected and manipulated with the approval of the Committee on Ethics of Experiments of the South-Central University for Nationalities, China (Permit Number: 2017-SCUEC-MEC-007).[40]

## Animal Care

In this study, animal care and usage followed the guidelines outlined in the Guide for Animal Experimentation of the South-Central University for Nationalities and the Committee of Research Facilities for Laboratory Animal Sciences of the South-Central University for Nationalities. The protocols used adhered to the guidelines for conducting animal studies and received approval from the Committee on the Ethics of Experiments of the South-Central University for Nationalities, China (Permit Number: 2016-SCUEC-AEC-003).[41] To minimize animal suffering, mice were sacrificed by $CO_2$ inhalation under anesthesia. Before the experiment, a total of 80 Kunming mice (males, 6–8 weeks old, initially weighing 18 to 22 g) were acclimated under specific pathogen-free (SPF) conditions for seven days.[42] Detailed experimental procedures and methods are provided in the Supplemental Files.

## Preparation of Nanosized Materials

To enhance the solubility and bioavailability of diethylnitrosamine (DEN), we utilized a nanoformulation termed nanoDEN, a typical N-nitrosamine. This nanoDEN formulation was chosen based on our previous studies demonstrating its ability to enhance oncogenesis and liver cancer development in mice.[41] NanoDEN was synthesized using a high-pressure microfluidics technique, which has been previously validated for its efficiency and reproducibility in generating nanoparticles with consistent size and properties. Detailed methods and parameters used for the synthesis of nanoDEN are provided in the Supplemental files.

## Experimental Design and Treatments

To investigate the synergistic effects of propionic testosterone (TP) and nanoDEN on liver carcinogenesis, 80 male Kunming mice were acclimated for a week and then housed in groups of four. Mice were randomly assigned to four groups: Normal group (n=20), Normal +TP group (n=20), NanoDEN group (n=20), and NanoDEN +TP group (n=20). The Normal +TP and NanoDEN +TP groups received intraperitoneal injections of TP at 375 mg/kg once a week for three weeks. The Normal, Normal +TP, NanoDEN, and NanoDEN +TP groups were orally administered 16.5 mg/kg (equivalent to 4WL/10g) of corn oil, corn oil, nanoDEN, and nanoDEN, respectively, once a week until the end of week 20. Mice were monitored daily for fur condition, diet, and activity. Weight was recorded weekly, and all mice had ad libitum access to food and water, with bedding changed every other day.

## Collection of Tissue Samples

Mice were euthanized at weeks 5, 10, 15, and 20 post-treatment. Liver tissues were immediately dissected, weighed, photographed, and assessed for morphology, color, and texture. The liver was rinsed in saline to remove surface blood. The liver tissue was then divided into two parts: one was fixed in 10% neutral formalin at room temperature for 24 hours

for histopathological examination, and the other was immediately stored in liquid nitrogen and subsequently kept at −80°C for Western blot analysis.

## Histopathological Analysis of Liver Tissues

The liver tissue was fixed in 10% neutral formalin, embedded in paraffin, sectioned at 4μm, and stained with hematoxylin and eosin (H&E) or Masson's trichrome using standard techniques. Histopathological examination of the liver sections was performed by pathologists using a Nikon 50i light microscope (Nikon, Tokyo, Japan).[41]

## Immunohistochemical Staining of Liver Tissues

Deparaffinized samples were hydrated, followed by 3% hydrogen peroxide blocking for 15 minutes. The specimens were then immersed in 0.01 M boiling citrate buffer and microwaved for one minute in order to extract antigens. Immediately following blocking with 5% BSA (Boster, Wuhan, China) for 40 minutes, the sections were incubated overnight at 4°C with primary antibodies against AR (1:100), β-catenin (1:100) and HMGB-1 (1:100), respectively. Samples were deparaffinized, hydrated, and blocked with 3% hydrogen peroxide for 15 minutes. Then slices were subjected to antigen retrieval by immersing in 0.01 M boiling citrate buffer and heating in a microwave oven for 1 minute. Sections were blocked by 5% BSA (Boster, Wuhan, China) for 40 minutes at room temperature, and further incubated with primary antibodies against AR (1:100), β-catenin (1:100), and HMGB-1 (1:100) at 4°C overnight, respectively.[28] Finally, expression of immunoreactivity was visualized by 3,3'-diaminobenzidine tetrahydrochloride (DAB; Boster, Wuhan, China) after process of incubating with horseradish peroxidase (HRP)-conjugated secondary antibodies (Boster, Wuhan, China) at 37°C for 40 minutes. Using hematoxylin as a nuclear counterstain, the slices were then dehydrated in a graded series of alcohol washes and mounted with coverslips.[41]

## Scoring System for Evaluating Liver Injury Severity and Index Calculation

In this study, we employed a comprehensive scoring system to gauge the severity of liver injury within our experimental models, which is grounded in histopathological assessments. This system scrutinizes specific attributes like hepatocellular necrosis and inflammation, hepatic fibrosis, and hepatic steatosis. Scores for hepatocellular necrosis and inflammation range from 0 (no evidence) to 3 (extensive damage), while fibrosis scores range from 0 (no evidence) to 3 (extensive fibrotic areas). For hepatic steatosis, scores vary from 0 (no evidence) to 3 (large aggregates of fat). Each attribute is assigned a score between 0 and 3, and a higher cumulative score denotes more severe liver injury. This scoring was carried out by three professional pathologists who were blinded to the experimental groups to ensure an impartial assessment of pathological alterations.

In addition to the histopathological scoring, we have integrated a detailed description of the formulas or methods used to calculate the liver index and injury index in the method section. This involves assigning scores to the severity of liver damage observed in tissue sections stained with hematoxylin and eosin (H&E staining). Each type of injury, such as hepatocellular necrosis, inflammation, and fibrosis, is given a score based on its severity, with 0 indicating absence, 1 for mild, 2 for moderate, and 3 for severe. The Injury Index (Histopathological Score) is then calculated as the total score of individual injuries divided by the total number of injuries. This additional detail provides clarity on how the liver and injury indices were calculated, ensuring transparency and reproducibility of our evaluation methods.

## Statistical Analysis

The expression and localization data of human and mouse samples were collected from at least nine different views of three different sample slices per sample. The means ± SEM were used to present data. GraphPad Prism 5.0.1 software package was used for the statistical analyses. The detailed methods for statistics were included in the Supplemental files. The significance between groups were calculated with two-tailed tests. † represents $p > 0.05$, and *** and *** represent significant difference with $p < 0.05$, 0.01 and 0.001, respectively.

# Results

## Food and Water Intake

During the course of the experiment, both the nanoDEN and nanoDEN + TP groups exhibited a reduction in food and water intake. However, the most significant decrease was observed in the nanoDEN + TP group, especially after week 15. Compared to the control and other treatment groups, the mice in the nanoDEN + TP group consumed markedly less food and water. This pronounced reduction in both food and water intake in the nanoDEN + TP group may indicate an overall decline in health or discomfort experienced by the animals.

## Testosterone Exacerbated Liver Damage and Tumor Formation in nanoDEN-Treated Mice

To investigate whether activation of AR could enhance tumor formation in mice, a liver tumor model was developed by treating mice with TP, a prototypical testosterone compound. As depicted in Figure 1, both the liver index and injury index were significantly exacerbated in the nanoDEN + TP group, compared to either the normal + TP group or the nanoDEN group.

It's crucial to note the time-dependent effects observed in our study. At week 15, significant associations were observed in both the nanoDEN + TP group and the nanoDEN group individually, suggesting that nanoDEN alone or in combination with TP contributed to liver tumor formation at this stage ($p < 0.05$). However, by week 20, the relationship between the nanoDEN + TP group and the TP-only group became non-significant ($p > 0.05$). Yet, the nanoDEN + TP group still showed a significant association with liver tumor formation when compared to the nanoDEN group ($p < 0.05$).

These findings suggest a possible dose-dependent effect of nanoDEN as the study progressed. With the increasing dosage of nanoDEN towards the end of the experiment, the influence of TP seemed to diminish, emphasizing the potency of nanoDEN in promoting liver tumor formation.

Furthermore, it is noteworthy that inflammation in liver tissues appeared earlier in the TP-injected nanoDEN group, indicating that TP not only intensifies tumor formation but also inflicts greater harm on the liver.

## Activation of AR Changed Expression Patterns of β-Catenin and HMGB1 During the Progression of Liver Tumor in Mice

To further investigate the relationship between different factors, liver samples from the aforementioned mice were collected and subjected to immunohistochemistry (IHC) staining. The results demonstrated that the expression of AR was elevated in the nanoDEN + TP group during the initial 15 weeks (Figure 2). However, in the liver samples obtained from mice at week 20, the cytosolic expression of AR in the nanoDEN group increased and showed no significant difference compared to the nanoDEN + TP group. In contrast, there was a significant upregulation of nuclear AR expression in the nanoDEN + TP group at week 20, surpassing all other three groups. These findings indicate a correlation between tumor formation and the elevation of nuclear AR expression, similar to what was observed in the human samples.

As illustrated in Figure 3, histochemical staining revealed distinct patterns of β-catenin expression in the liver samples. Specifically, the nuclear expression of β-catenin was significantly increased in the nanoDEN + TP group compared to the TP-only group during the 5th and 20th weeks. However, it remained relatively low in both groups during the 10th and 15th weeks. Conversely, a slight elevation in cytosolic expression of β-catenin was observed in the nanoDEN + TP group during the 10th week, but this pattern dissipated in the subsequent weeks.

The nuclear localization of HMGB1 showed a unique pattern across the treatment groups, as demonstrated in Figure 4. Upon TP administration, nuclear HMGB1 expression increased in both the TP and nanoDEN + TP groups during the 10th week. Subsequently, its nuclear expression decreased in the 15th and 20th weeks, although the levels still surpassed those in the TP untreated groups during the 15th week. Notably, nanoDEN treatment led to an increase in nuclear HMGB1 expression in the 20th week. The correlations between AR, β-catenin, and HMGB1 are summarized in Table S1. Specifically, the expression of AR correlated strongly with cytoplasmic β-catenin in the mice during the 5th week, while β-catenin showed a strong correlation with nuclear HMGB1 in the 10th week. Furthermore, the expression patterns of these factors were confirmed by Western blot analysis, as depicted in Figure S1.

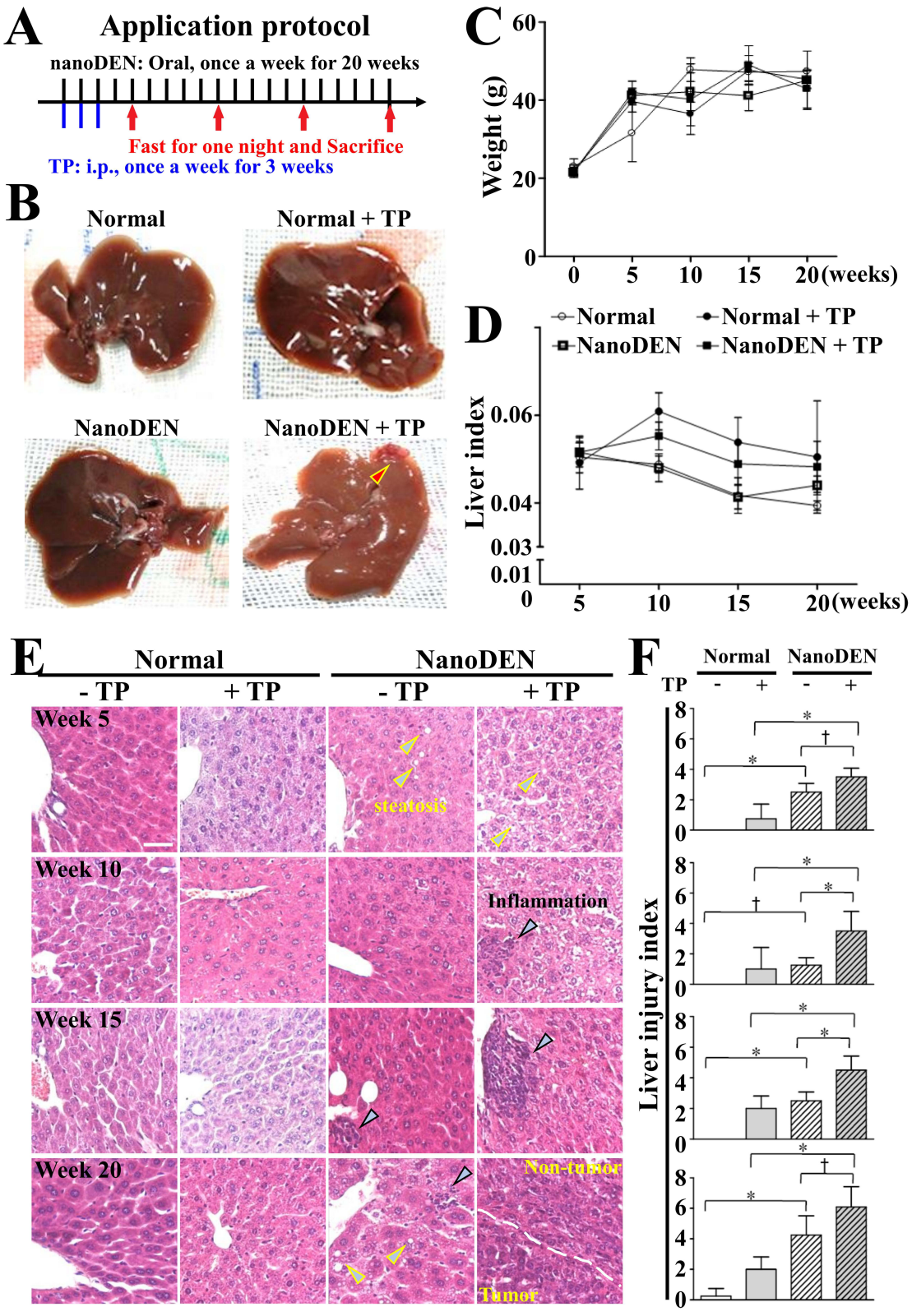


**Figure 1** TP exacerbated liver damage and tumor formation in nanoDEN-treated mice.

**Notes**: (**A**) The application protocol for mice model establishment. (**B**) Representative graphs of liver samples collected from mice. Red arrow indicated a tumor observed in the nanoDEN + TP group. (**C**) The weights of livers in different groups of mice. (**D**) The liver indices in different groups of mice. (**E**) H&E staining of liver samples from mice. Inflammation was indicated by black arrows; steatosis was indicated by yellow arrows; non-tumor or tumor areas were split by white dashes. Scale bar, 50 μm. (**F**) The summary of liver injury indices of liver samples from mice. n = 5 per group. * represents significant difference with $p < 0.05$, while † represents $p > 0.05$.

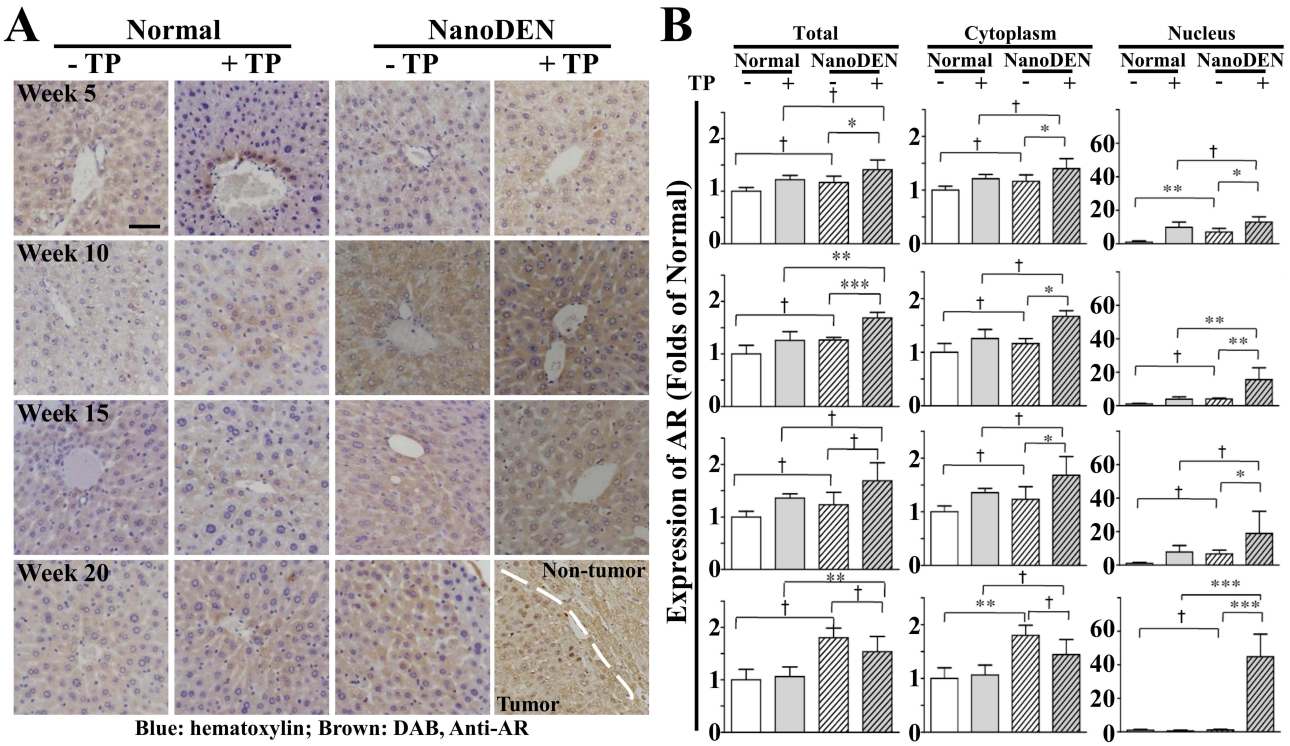


**Figure 2** Nuclear expression of AR was significantly elevated after TP injection in nanoDEN-treated mice.
**Notes**: (**A**) Representative graphs showing IHC staining patterns of AR expression in liver samples of nanoDEN-treated mice. Scale bar, 50 μm. Non-tumor or tumor areas were split by white dashes. (**B**) The summary of expressions of AR in liver samples of nanoDEN-treated mice. n = 5 per group. *, ** and *** represents significant difference with $p < 0.05$, 0.01 and 0.001, respectively, while † represents $p > 0.05$.

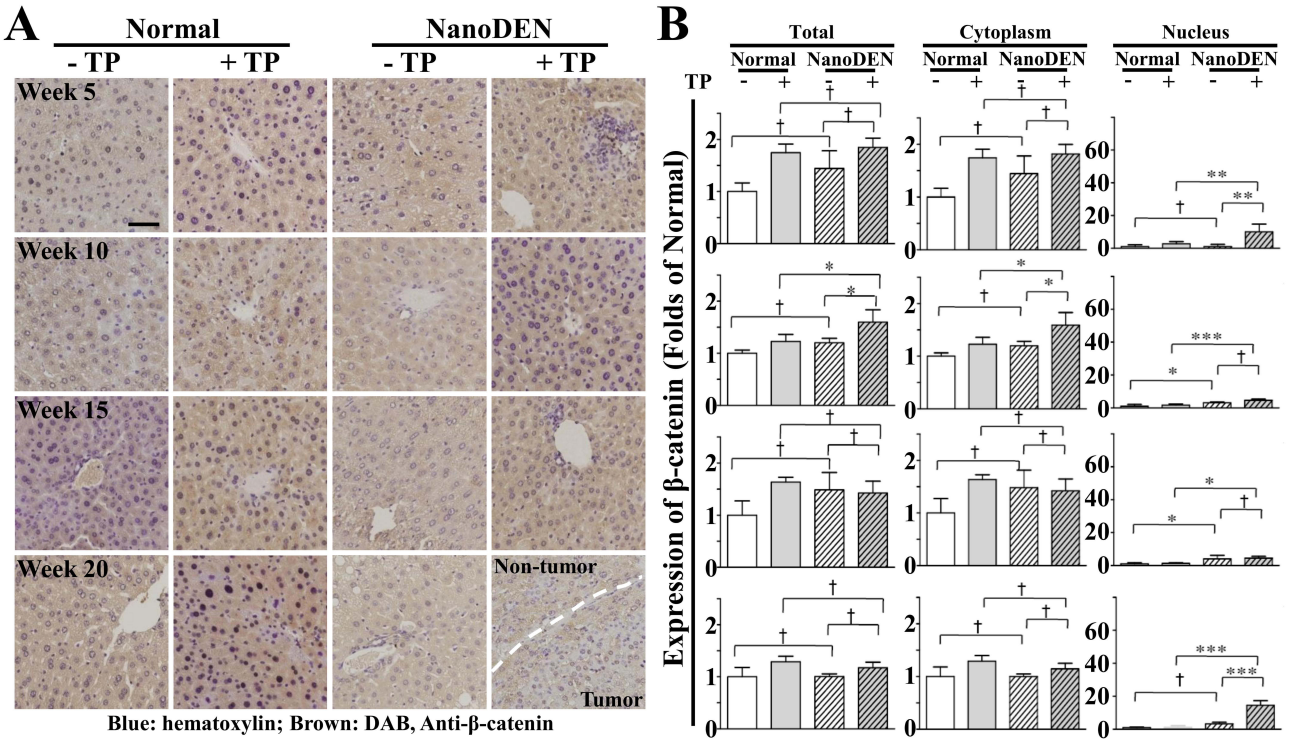


**Figure 3** Nuclear expression of β-catenin was significantly elevated after TP injection in nanoDEN-treated mice.
**Notes**: (**A**) Representative graphs showing IHC staining patterns of β-catenin expression in liver samples of nanoDEN-treated mice. Scale bar, 50 μm. Non-tumor or tumor areas were split by white dashes. (**B**) The summary of expressions of β-catenin in liver samples of nanoDEN-treated mice. n = 5 per group. *, ** and *** represents significant difference with $p < 0.05$, 0.01 and 0.001, respectively, while † represents $p > 0.05$.


https://doi.org/10.2147/OTT.S456746 DovePress

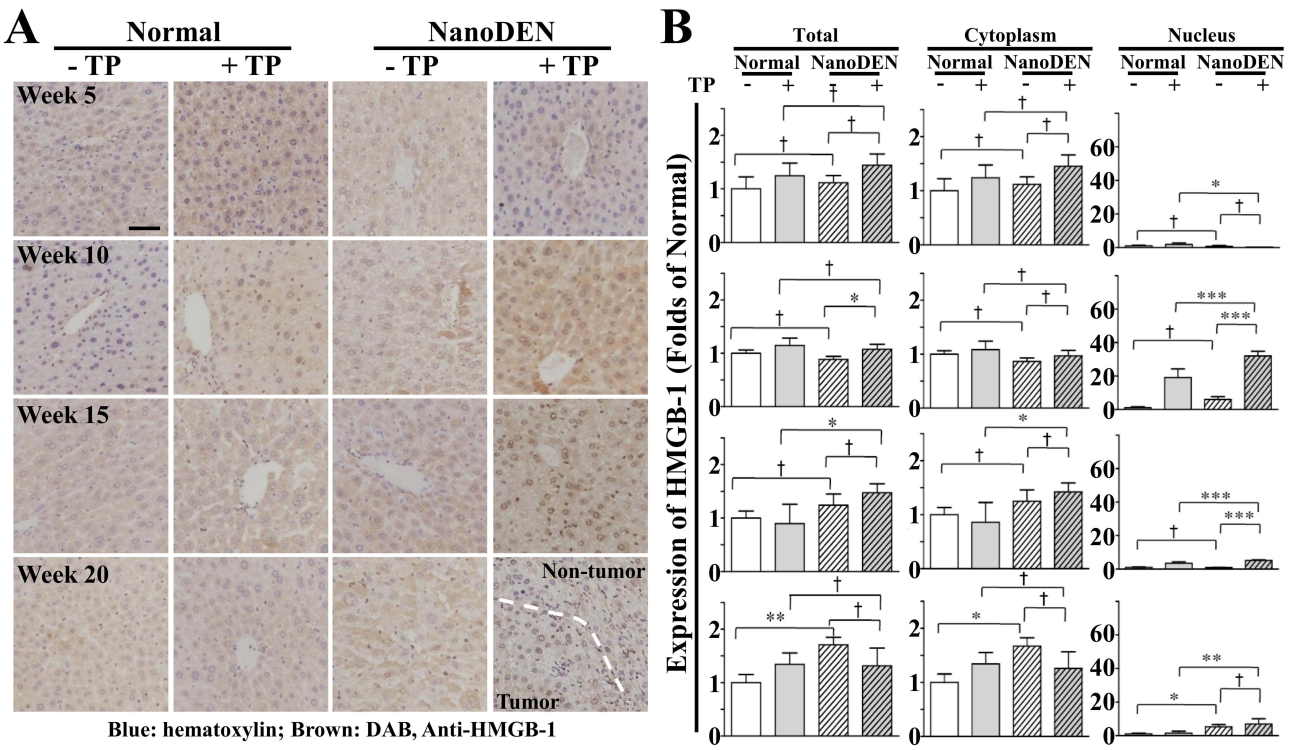


**Figure 4** Nuclear expression of HMGB-1 was significantly elevated after TP injection in nanoDEN-treated mice.
**Notes**: (**A**) Representative graphs showing IHC staining patterns of HMGB1 expression in liver samples of nanoDEN-treated mice. Scale bar, 50μm. Non-tumor or tumor areas were split by white dashes. (**B**) The summary of expressions of HMGB-1 in liver samples of nanoDEN-treated mice. n = 5 per group. *, ** and *** represents significant difference with $p < 0.05$, 0.01 and 0.001, respectively, while † represents $p > 0.05$.

These results indicate that the administration of TP effectively promoted the nuclear localization of AR, thereby facilitating the nuclear localization of β-catenin during the initial stages of TP treatment and tumor formation. Concurrently, TP treatment also enhanced the nuclear localization of HMGB-1 in the early phase of liver damage.

## The Expressions of AR, β-Catenin and HMGB1 Were Different in Non-Tumor or Tumor Areas in Liver Samples of Mice

To further verify our findings, we analyzed the expression and patterns of these three pivotal factors in non-tumor or tumor areas of liver samples from mice at week 20. The results corresponding to the 20th week are presented in Figure 5. Notably, the correlations between these factors were calculated and summarized in Table S2, which showed a positive correlation between AR and β-catenin in the nucleus of tumor areas, and between AR and HMGB-1 in the cytoplasm of non-tumor areas.

## The Expressions of AR, β-Catenin and HMGB1 Were Different in Non-Tumor or Tumor Areas in Liver Samples of HCC Patients

In order to investigate whether the expressions of pivotal factors, such as AR, β-catenin, and HMGB1, were altered in the livers of HCC patients, we collected 34 liver samples and performed histopathological analysis. As depicted in Figure 6, the protein expression of cytoplasm-localized AR did not show significant differences between tumor and non-tumor areas. However, there was a notable increase in the nuclear localization of AR, with a significantly higher rate observed in the tumor areas. For β-catenin, both cytoplasmic and nuclear expressions were significantly up-regulated. Although the rate of nuclear localization showed an increase, the difference in enhancement between averages was not substantial. In contrast, the expression of HMGB1 decreased in the cytoplasm but increased in the nucleus, resulting in a significant rise in the rate of nuclear localization.

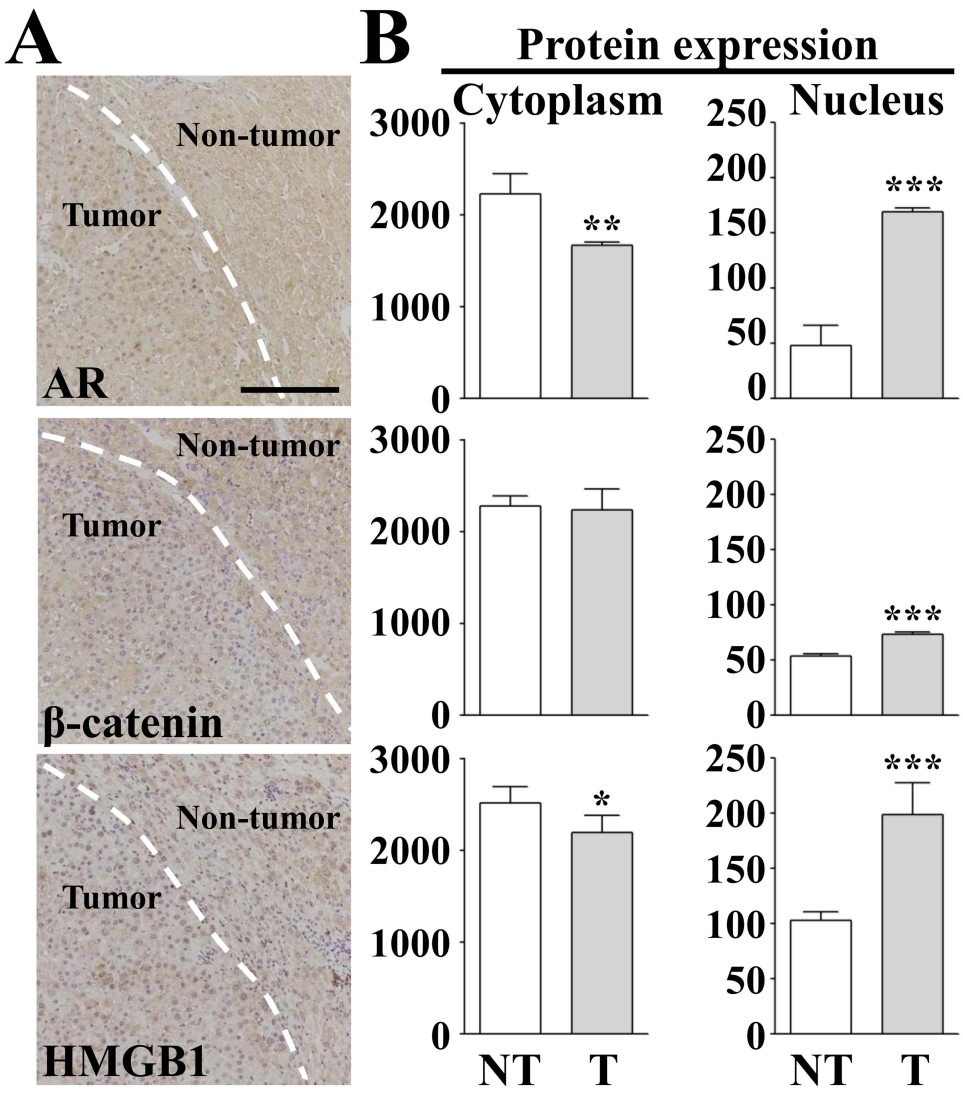


**Figure 5** The expressions of AR, β-catenin and HMGB-1 were different in non-tumor or tumor areas in liver samples of mice. (**A**).
**Notes**: (**A**) Representative graphs of IHC staining of AR, β-catenin and HMGB-1 in non-tumor or tumor areas of liver samples from mice. Scale bar, 50 μm. Non-tumor or tumor areas were split by white dashes. (**B**) The summary of the cytosolic and nuclear expressions of proteins in non-tumor or tumor areas of liver samples from mice. n = 5 per group. *, ** and *** represents significant difference with $p < 0.05$, 0.01 and 0.001, respectively.

To investigate the correlations among these factors in liver samples, we utilized the Pearson correlation coefficient. The results, depicted in Figure 7, indicated that the expression pattern of AR was, at least partially, correlated with that of HMGB-1 in the non-tumor area, while the expression pattern of AR was correlated with that of β-catenin in the tumor area. These findings suggest that the activation and nuclear localization of AR could potentially influence the expression patterns of both β-catenin and HMGB-1, thereby impacting the development of liver cancer. These results are consistent with our findings from animal experiments.

After analyzing the expression levels of AR, β-catenin, and HMGB-1 in liver samples from HCC patients, we further examined the correlations between these protein expressions and various clinical factors. Table S3 summarizes the correlations between protein overexpression and different clinical parameters, including sex, age, tumor size, encapsulation, and tumor differentiation.

## Discussion

N-nitrosamines are widely recognized as carcinogens in our daily lives.[13] The carcinogenic potential of N-nitrosamines was first reported approximately 80 years ago in 1937 when it was discovered that dimethylnitrosamine (DMN) could induce liver

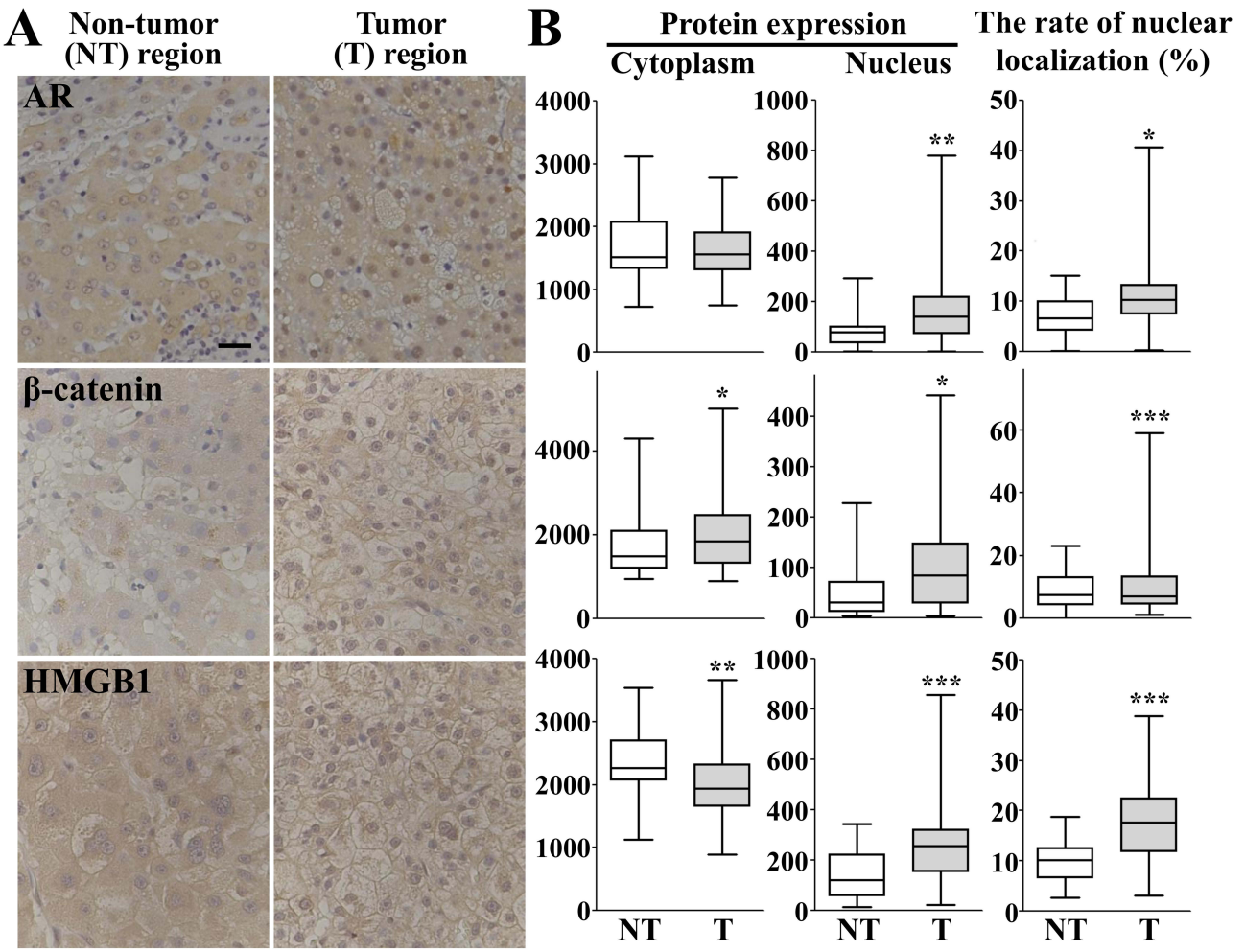


**Figure 6** The expressions of AR, β-catenin and HMGB1 in the cytoplasmic or nuclear regions of the non-tumor or tumor areas in liver samples of HCC patients.
**Notes**: (**A**) Representative graphs of immunohistochemical staining (Blue: haematoxylin; Brown: DAB, antibody for indicated proteins) in liver samples of HCC patients. Scale bar, 50 μm. (**B**) Summary data of (**A**). n = 34 pairs of samples. *, ** and *** represents significant difference with $p < 0.05$, 0.01 and 0.001, respectively.

damage in humans.[43] Since then, N-nitrosamines have been widely acknowledged as potent environmental carcinogens associated with liver damage and HCC development.[44] However, the hepatotoxicity of N-nitrosamines varies due to factors such as genetic background, sex, and age of the mice. Despite the variability, the role of N-nitrosamines in liver carcinogenesis is significant, especially considering our findings that co-exposure to TP exacerbates liver tumor formation following nanoDEN exposure through the activation of AR (the male hormonal receptor). Our experiments underscore the importance of timing in the progression of liver tumors. Early exposure to TP acts as a risk factor, accelerating liver damage processes like hepatitis, steatosis, and cancer formation. These observations align with previous studies suggesting a potential link between decreased testosterone levels and the progression of liver fibrosis to cancer.[45–47]

Epidemiological data consistently reveals a higher prevalence of liver cancer in males than females. Our study further elucidates this by demonstrating a close correlation among AR, β-catenin (a key molecule in the Wnt signaling pathway), and HMGB1 (a non-histone chromatin-associated protein involved in various cancers) in both human and mouse liver cancer samples. Importantly, our nanoDEN-induced liver cancer model allows us to assess the expression patterns of these factors over time, revealing dynamic interactions among them that occur in a time-dependent manner.

β-catenin, a key molecule in the Wnt/Frizzled signaling pathway, has been extensively studied in various cancers, including HCC.[48] In line with this, we identified a potential link between AR and β-catenin during liver tumor formation, particularly in the nucleus of tumorous areas in both human and mouse samples. It is worth noting that while nuclear expression of AR continuously increased, nuclear expression of β-catenin initially decreased for the first 10 weeks but

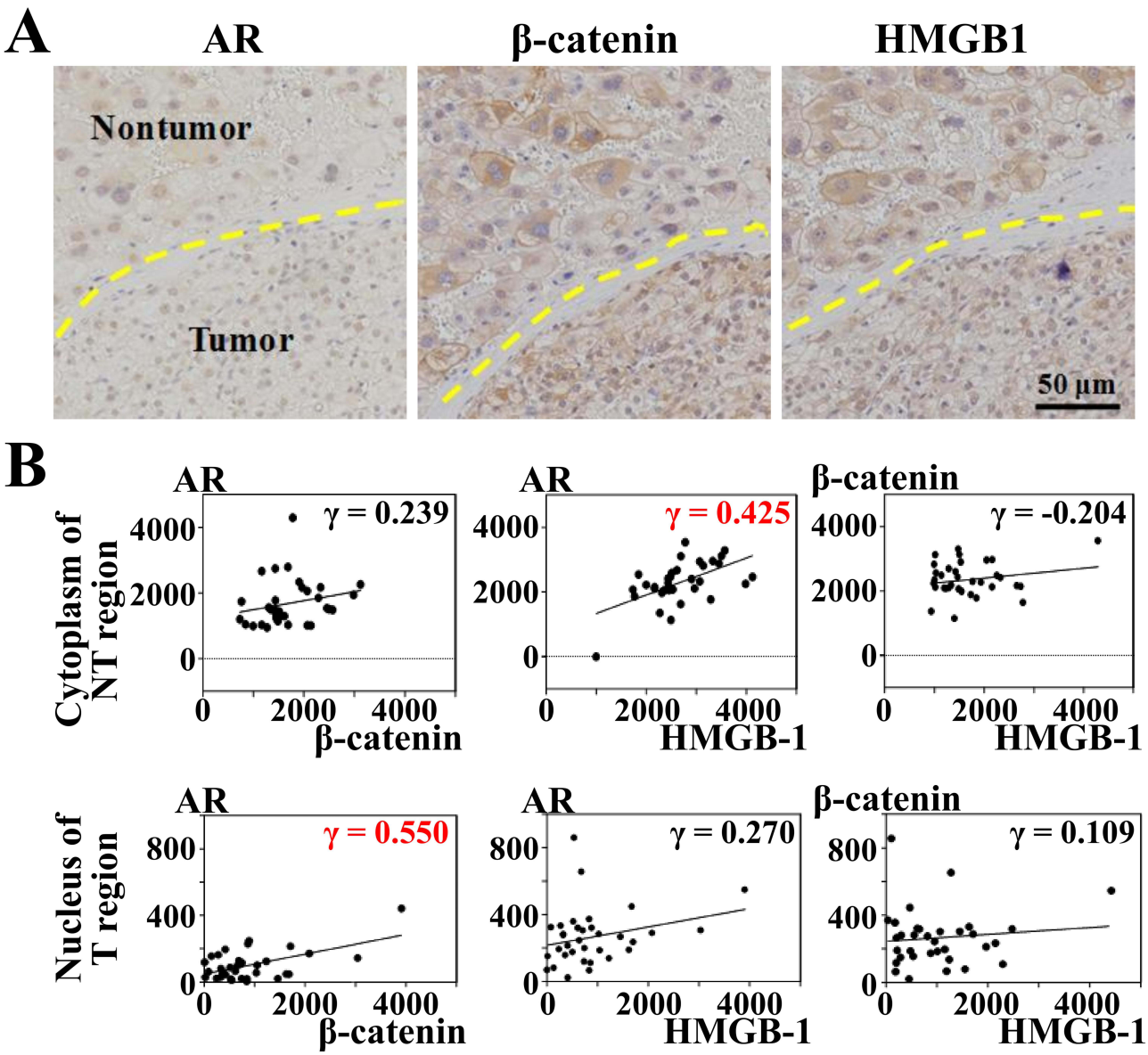


**Figure 7** The correlations between the expressions of AR, β-catenin and HMGB1 in the cytoplasmic or nuclear regions of the non-tumor or tumor areas in liver samples of HCC patients.

**Notes**: (**A**) Representative graphs showing the differences of staining patterns between non-tumor or tumor areas in liver samples of HCC patients. Scale bar, 50 μm. (**B**) The correlations between the expressions of AR, β-catenin and HMGB1. The Pearson's correlation co-efficiencies were indicated on the right corner, possible correlations were indicated as red. n = 34 pairs of samples.

showed an increase in the latter 10 weeks, suggesting the involvement of other signaling molecules and the potential bidirectional regulation by AR in different phases of oncogenesis.

It is widely acknowledged that AR plays vital roles in the development of male reproductive tissues, promotion of secondary sexual characteristics, and normal bodily functions such as growth, metabolism, and brain development. Recent studies have linked AR overexpression to various pathways in HCC cell lines or patients, including the Akt/mTOR pathway,[49] the pSTAT3/pAKT/pERK pathways[50] and transcriptional factor activity of ETS-1.[51] However, the effect of AR activation through its endogenous ligands, such as TP (the propionate form of testosterone), during the progression of HCC remains uninvestigated.

Early studies have demonstrated that HMGB1 can enhance the DNA binding ability of hormone receptors, including AR.[46,52,53] However, the relationship between HMGB1 and AR in HCC remains unclear. In our study, we observed

positive correlations between HMGB1 and AR in both human HCC and mice liver cancer samples. Notably, these correlations were primarily observed in the cytosol of tumor-adjacent regions (or non-tumor areas as previously indicated). Since HMGB1 is closely associated with the migration and invasion of cancer cells, our findings provide new insights into a potential regulatory mechanism in tumor formation.

The observed time-dependent changes in the expression of AR, β-catenin, and HMGB1 provide valuable insights into the dynamic nature of these proteins during liver tumorigenesis. In the initial stages of TP treatment and tumor induction, there was a notable elevation in the expression of AR in the nanoDEN + TP group, particularly during the first 15 weeks. This increase in AR expression was concurrent with an upregulation in the nuclear expression of β-catenin. Notably, the nuclear localization of HMGB1 also exhibited an increase during the 10th week following TP administration.

We emphasized the role of N-nitrosamines in liver carcinogenesis is significant, especially considering our findings that co-exposure to TP exacerbates liver tumor formation following nanoDEN exposure through the activation of AR, particularly during the first 15 weeks. This increase in AR expression was concurrent with an upregulation in the nuclear expression of β-catenin. Notably, the nuclear localization of HMGB1 also exhibited an increase during the 10th week following TP administration. Our nanoDEN-induced liver cancer model enabled us to assess the expression patterns of AR, β-catenin, and HMGB1 during liver tumor progression, revealing their dynamic interactions.

At the same time, our current understanding of oncogenesis primarily relies on data obtained from tumor-bearing mice. This preference for tumor-bearing mice stems from several advantages: they are easier to handle, allowing for faster experimental achievement than conventional primary liver cancer models, which simplifies the experimental procedure. It's also easier to control the tissue origin of tumors in these mice, requiring fewer clarifications regarding the complexity of tumor formation. Additionally, tumor-bearing mice often exhibit higher tumor growth rates and aggressiveness, making them effective "filters" for eliminating less potent candidates of pathways and drugs. However, a significant drawback of using these models is the lack of information before and during tumor formation. In contrast, the information gained from primary liver cancer models perfectly fills this information gap, providing a more comprehensive understanding of liver cancer development and its mechanisms.

In our study using human samples, we observed that the overall expression of AR did not vary significantly between tumorous and non-tumorous areas. Instead, the subcellular localization of AR played a more crucial role in liver tumor progression. This finding was further confirmed in our mouse model. After TP injection, we observed an increase in AR expression, which subsequently translocated into the nucleus. This led to enhanced formation of DEN-induced primary liver tumors in mice. Notably, we also observed that co-exposure to TP and nanoDEN significantly intensified the nuclear localization of AR in week-20 mice compared to the TP-alone group or the nanoDEN-alone group, indicating possible synergy during carcinogenesis.

As the study progressed, by week 20, a shift in the expression patterns was observed. While the cytosolic expression of AR in the nanoDEN group became comparable to the nanoDEN + TP group, a significant upregulation of nuclear AR was still evident in the nanoDEN + TP group. Similarly, the nuclear expression of β-catenin remained elevated in the nanoDEN + TP group during the 5th and 20th weeks, with a transient elevation in cytosolic expression during the 10th week. The nuclear expression of HMGB1 showed a decline in subsequent weeks but remained higher than the TP untreated groups. Interestingly, these time-dependent changes also influenced the correlation patterns among these proteins. In the initial stages, AR expression correlated strongly with cytoplasmic β-catenin, whereas β-catenin exhibited a strong correlation with nuclear HMGB1. However, by week 20, the relationship between these proteins shifted, indicating a dynamic interplay between AR, β-catenin, and HMGB1 during the progression of liver tumor formation.

Furthermore, the observed differences in the expression of these proteins between non-tumor and tumor areas further emphasize their role in liver tumorigenesis. In the tumor areas, a positive correlation was observed between nuclear AR and β-catenin, while in non-tumor areas, AR showed a strong correlation with cytoplasmic HMGB1. These findings highlight the complex and interconnected pathways involving AR, β-catenin, and HMGB1 in liver cancer development.

In summary, our study reveals intricate time-dependent changes in the expression of AR, β-catenin, and HMGB1 during liver tumor formation. These findings underscore the importance of understanding the temporal dynamics of these proteins in deciphering their roles and interactions in liver tumorigenesis. The correlation patterns and expression

changes observed provide valuable insights into the molecular mechanisms underlying liver cancer progression, potentially paving the way for targeted therapeutic interventions.

## Conclusion

In summary, this study provides evidence confirming that testosterone can worsen the development of liver cancer induced by exposure to environmental N-nitrosamines. Histopathological and immunohistochemical staining experiments have revealed strong correlations between AR and β-catenin in the nuclear region of tumor areas, as well as between AR and HMGB1 in the cytoplasmic region of non-tumor areas, in both human and mouse samples. Furthermore, the study has demonstrated the time-dependent expression levels and patterns of these three proteins during the progression of liver tumors. These findings support the notion that AR can regulate the expression levels and patterns of β-catenin and HMGB1 in vivo, thereby exacerbating the progression of liver cancer induced by exposure to environmental N-nitrosamines. There-fore, understanding the hepatotoxicity caused by combined exposure to N-nitrosamines and testosterone, along with its underlying mechanism, holds significant importance for ensuring drug safety in clinical practice and environmental safety by reducing N-nitrosamines exposure through conscious choices in diet and lifestyle.

## Data Sharing Statement

The data used to support the findings of this study are available from the corresponding author upon request.

## Institutional Review Board Statement

All animal experiments were approved by the Ethics Committee of the South-Central University for Nationalities for the use of animals and conducted in accordance with the National Institutes of Health Laboratory Animal Care and Use Guidelines.All research on mice was approved by the Animal Experiment Ethics Committee of the South-Central University for Nationalities, Wuhan, China (permit number: 2019-SCUEC-AEC-013).

## Acknowledgments

We would like to thank the specialists and the staff members for involved in the research for their valuable advice.

## Funding

This work was funded by the National Natural Science Foundation of China (82174110, 81673711, 81573887) and by the Health Research Foundation of Wuhan Municipal Health Commission, China (WZ19A16).

## Disclosure

The authors report no conflicts of interest in this work.

## References

1. Li YY, Wan MM, Zhu JH. Cleaning carcinogenic nitrosamines with zeolites. *Environ Chem Lett*. 2014;12(1):139–152. doi:10.1007/s10311-013-0451-1
2. Lona-Ramirez FJ, Gonzalez-Alatorre G, Rico-Ramírez V, Perez-Perez MC, Castrejón-González EO. Gas chromatography/mass spectrometry for the determination of nitrosamines in red wine. *Food Chem*. 2016;196:1131–1136. doi:10.1016/j.foodchem.2015.09.090
3. Li X, Bei E, Qiu Y, et al. Intake of volatile nitrosamines by Chinese residents in different provinces via food and drinking water. *Sci Total Environ*. 2021;1(754):142121. doi:10.1016/j.scitotenv.2020.142121
4. Ramírez N, Özel MZ, Lewis AC, Marcé RM, Borrull F, Hamilton JF. Exposure to nitrosamines in thirdhand tobacco smoke increases cancer risk in non-smokers. *Environ Int*. 2014;71:139–147. doi:10.1016/j.envint.2014.06.012
5. Wu CC, Wang WJ, Bao LJ, Shi L, Tao S, Zeng EY. Impacts of texture properties and airborne particles on accumulation of tobacco-derived chemicals in fabrics. *J Hazard Mater*. 2019;369:108–115. doi:10.1016/j.jhazmat.2018.12.107
6. Chen Y, Chen W, Huang H, et al. Occurrence of N-nitrosamines and their precursors in the middle and lower reaches of Yangtze River water. *Environ. Res*. 2021;195:110673. doi:10.1016/j.envres.2020.110673
7. Luo Q, Bei E, Liu C, et al. Spatial, temporal variability and carcinogenic health risk assessment of nitrosamines in a drinking water system in China. *Sci Total Environ*. 2020;736:139695. doi:10.1016/j.scitotenv.2020.139695
8. Fan CC, Lin TF. N-nitrosamines in drinking water and beer: detection and risk assessment. *Chemosphere*. 2018;200:48–56. doi:10.1016/j.chemosphere.2018.02.025

9. Farren NJ, Ramírez N, Lee JD, Finessi E, Lewis AC, Hamilton JF. Estimated Exposure Risks from Carcinogenic Nitrosamines in Urban Airborne Particulate Matter. *Enviro Sci Technol*. 2015;49(16):9648–9656. doi:10.1021/acs.est.5b01620
10. Choi NR, Ahn YG, Lee JY, et al. Winter-time particulate nitrosamines and nitramines in the atmosphere at Seoul, South Korea. *Atmos Environ*. 2020;237:117582. doi:10.1016/j.atmosenv.2020.117582
11. Engemann A, Focke C, Humpf H-U. Intestinal Formation of N -Nitroso Compounds in the Pig Cecum Model. *J Agr Food Chem*. 2013;61 (4):998–1005. doi:10.1021/jf305040e
12. Kobayashi J. Effect of diet and gut environment on the gastrointestinal formation of N-nitroso compounds: a review. *Nitric Oxide*. 2018;73:66–73. doi:10.1016/j.niox.2017.06.001
13. Gushgari AJ, Halden RU. Critical review of major sources of human exposure to N-nitrosamines. *Chemosphere*. 2018;210:1124–1136. doi:10.1016/j.chemosphere.2018.07.098
14. Li YS, Leng CL, Chen MT, et al. Mouse hepatic neoplasm formation induced by trace level and low frequency exposure to diethylnitrosamine through β-catenin signaling pathway. *Toxicol Res*. 2016;5(1):210–223. doi:10.1039/c5tx00317b
15. McGuire S. World Cancer Report 2014. Geneva, Switzerland: world Health Organization, International Agency for Research on Cancer, WHO Press, 2015. *Adv. Nutr.* 2016;7(2):418–419. doi:10.3945/an.116.012211
16. Paula Santos N, Colaço A, da Costa RM G, Manuel Oliveira M, Peixoto F, Alexandra Oliveira P. N-diethylnitrosamine mouse hepatotoxicity: time-related effects on histology and oxidative stress. *Exp Toxicol Pathol*. 2014;66(9–10):429–436. doi:10.1016/j.etp.2014.07.002
17. Zheng B, Zhu YJ, Wang HY, Chen L. Gender disparity in hepatocellular carcinoma (HCC): multiple underlying mechanisms. *Sci China Life Sci*. 2017;60(6):575–584. doi:10.1007/s11427-016-9043-9
18. El-Serag HB, Rudolph KL. Hepatocellular carcinoma: epidemiology and molecular carcinogenesis. *Gastroenterology*. 2007;132(7):2557–2576. doi:10.1053/j.gastro.2007.04.061
19. Ruggieri A, Barbati C, Malorni W. Cellular and molecular mechanisms involved in hepatocellular carcinoma gender disparity. *Int j Cancer*. 2010;127(3):499–504. doi:10.1002/ijc.25298
20. Lee C, Kim J, Han J, et al. Formyl peptide receptor 2 determines sex-specific differences in the progression of nonalcoholic fatty liver disease and steatohepatitis. *Nat Commun*. 2022;13(1):578. doi:10.1038/s41467-022-28138-6
21. Sinclair M, Grossmann M, Gow PJ, Angus PW. Testosterone in men with advanced liver disease: abnormalities and implications. *J Gastroenterol Hepatol*. 2015;30(2):244–251. doi:10.1111/jgh.12695
22. Bao S, Jin S, Wang C, Tu P, Hu K, Lu J. Androgen receptor suppresses vasculogenic mimicry in hepatocellular carcinoma via circRNA7/miRNA7-5p/VE-cadherin/Notch4 signalling. *J Cell Mol Med*. 2020;24(23):14110–14120. doi:10.1111/jcmm.16022
23. Ma WL, Hsu CL, Wu MH, et al. Androgen receptor is a new potential therapeutic target for the treatment of hepatocellular carcinoma. *Gastroenterology*. 2008;135(3):947–55, 955.e1–5. doi:10.1053/j.gastro.2008.05.046
24. Ao J, Meng J, Zhu L, et al. Activation of androgen receptor induces ID1 and promotes hepatocellular carcinoma cell migration and invasion. *Mol Oncol*. 2012;6(5):507–515. doi:10.1016/j.molonc.2012.06.005
25. Gioeli D, Ficarro SB, Kwiek JJ, et al. Androgen receptor phosphorylation. Regulation and identification of the phosphorylation sites. *J Biol Chem*. 2002;277(32):29304–29314. doi:10.1074/jbc.M204131200
26. Sharma V, Thangaraj K, Jyothy A. A novel insertion-induced frameshift mutation of the androgen receptor gene in a patient with primary amenorrhea. *Meta Gene*. 2014;2:11–15. doi:10.1016/j.mgene.2013.10.011
27. Wasmuth EV, Broeck AV, LaClair JR, et al. Allosteric interactions prime androgen receptor dimerization and activation. *Molecular Cell*. 2022;82 (11):2021–2031.e5. doi:10.1016/j.molcel.2022.03.035
28. Feng H, Cheng AS, Tsang DP, et al. Cell cycle-related kinase is a direct androgen receptor-regulated gene that drives β-catenin/T cell factor-dependent hepatocarcinogenesis. *J Clin Invest*. 2011;121(8):3159–3175. doi:10.1172/jci45967
29. Zhao L, Jin Y, Donahue K, et al. Tissue Repair in the Mouse Liver Following Acute Carbon Tetrachloride Depends on Injury-Induced Wnt/β-Catenin Signaling. *Hepatology*. 2019;69(6):2623–2635. doi:10.1002/hep.30563
30. Ando A, Hashimoto N, Sakamoto K, et al. Repressive role of stabilized hypoxia inducible factor 1α expression on transforming growth factor β-induced extracellular matrix production in lung cancer cells. *Cancer Science*. 2019;110(6):1959–1973. doi:10.1111/cas.14027
31. Mandke P, Vasquez KM. Interactions of high mobility group box protein 1 (HMGB1) with nucleic acids: implications in DNA repair and immune responses. *DNA Repair*. 2019;83:102701. doi:10.1016/j.dnarep.2019.102701
32. Iachettini S, Ciccarone F, Maresca C, et al. The telomeric protein TERF2/TRF2 impairs HMGB1-driven autophagy. *Autophagy*. 2023;19 (5):1479–1490. doi:10.1080/15548627.2022.2138687
33. Yang H, Wang H, Andersson U. Targeting Inflammation Driven by HMGB1. *Front Immunol*. 2020;11:484. doi:10.3389/fimmu.2020.00484
34. Klune JR, Dhupar R, Cardinal J, Billiar TR, Tsung A. HMGB1: endogenous danger signaling. *Mol Med*. 2008;14(7–8):476–484. doi:10.2119/2008-00034.Klune
35. Xu X, Piao HN, Aosai F, et al. Arctigenin protects against depression by inhibiting microglial activation and neuroinflammation via HMGB1/TLR4/NF-κB and TNF-α/TNFR1/NF-κB pathways. *Br J Pharmacol*. 2020;177(22):5224–5245. doi:10.1111/bph.15261
36. Liu Y, Chen L, Gao L, et al. LRRK2 deficiency protects the heart against myocardial infarction injury in mice via the P53/HMGB1 pathway. *Free Radic Biol Med*. 2022;191:119–127. doi:10.1016/j.freeradbiomed.2022.08.035
37. Ren Y, Cao L, Wang L, et al. Autophagic secretion of HMGB1 from cancer-associated fibroblasts promotes metastatic potential of non-small cell lung cancer cells via NFκB signaling. *Cell Death Dis*. 2021;12(10):858. doi:10.1038/s41419-021-04150-4
38. Huang Q, Liu J, Shi Z, Zhu X. Correlation of MMP-9 and HMGB1 expression with the cognitive function in patients with epilepsy and factors affecting the prognosis. *Cell Mol Biol*. 2020;66(3):39–47.
39. Zou M, Dong H, Meng X, et al. Store-operated Ca2+ entry plays a role in HMGB1-induced vascular endothelial cell hyperpermeability. *PLoS One*. 2015;10(4):e0123432. doi:10.1371/journal.pone.0123432
40. Qin QF, Li XJ, Li YS, et al. AMPK-ERK/CARM1 Signaling Pathways Affect Autophagy of Hepatic Cells in Samples of Liver Cancer Patients. *Front Oncol*. 2019;9:1247. doi:10.3389/fonc.2019.01247
41. Zhang WK, Gu HW, Li XJ, et al. The dark side of "the force" - lipid nanoparticles enhance the oncogenesis of diethylnitrosamine and result in liver cancer in mice. *Nanomedicine*. 2017;13(2):701–711. doi:10.1016/j.nano.2016.09.017

42. Chen XZ, Zhang WK, Tang HB, et al. The Ethanol Supernatant Extracts of Liushenwan Could Alleviate Nanodiethylnitrosamine-Induced Liver Cancer in Mice. *Can J Gastroenterol Hepatol*. 2018;2018:6934809. doi:10.1155/2018/6934809
43. Freund HA. Clinical manifestations and studies in parenchymatous hepatitis. *Ann Intern Med*. 2023;10:1144–1155.
44. Sheweita SA, El Banna YY, Balbaa M, Abdullah IA, Hassan HE. N-nitrosamines induced infertility and hepatotoxicity in male rabbits. *Environ. Toxicol.* 2017;32(9):2212–2220. doi:10.1002/tox.22436
45. Bassil N, Alkaade S, Morley JE. The benefits and risks of testosterone replacement therapy: a review. *Therapeutics Clin Risk Management*. 2009;5 (3):427–448. doi:10.2147/tcrm.s3025
46. Likos E, Bhattarai A, Weyman CM, Shukla GC. The androgen receptor messenger RNA: what do we know? RNA biology. *Jan*. 2022;19 (1):819–828. doi:10.1080/15476286.2022.2084839
47. Abdel-Hamid NM, Al-Quzweny RM. Prevalence of Hepatocellular Carcinoma in Men and the Contribution of Androgen and its Receptor in Pathogenesis and Therapy. *Curr Mol Pharmacol*. 2023;16(5):559–563. doi:10.2174/1874467215666221010092825
48. Meng Z, Liu Q, Liu Y, Yang Y, Shao C, Zhang S. Frizzled-3 suppression overcomes multidrug chemoresistance by Wnt/β-catenin signaling pathway inhibition in hepatocellular carcinoma cells. *J Chemother*. 2023;1–9. doi:10.1080/1120009x.2023.2182573
49. Zhang H, Li XX. Significance and mechanism of androgen receptor overexpression and androgen receptor/mechanistic target of rapamycin cross-talk in hepatocellular carcinoma. *Hepatology*. 2018;67(6):2271–2286. doi:10.1002/hep.29715
50. Xu J, Zheng L, Chen J, et al. Increasing AR by HIF-2α inhibitor (PT-2385) overcomes the side-effects of sorafenib by suppressing hepatocellular carcinoma invasion via alteration of pSTAT3, pAKT and pERK signals. *Cell Death Dis*. 2017;8(10):e3095. doi:10.1038/cddis.2017.411
51. Ren H, Ren B, Zhang J, et al. Androgen enhances the activity of ETS-1 and promotes the proliferation of HCC cells. *Oncotarget*. 2017;8 (65):109271–109288. doi:10.18632/oncotarget.22669
52. Boonyaratanakornkit V, Melvin V, Prendergast P, et al. High-mobility group chromatin proteins 1 and 2 functionally interact with steroid hormone receptors to enhance their DNA binding in vitro and transcriptional activity in mammalian cells. *Mol Cell Biol*. 1998;18(8):4471–4487. doi:10.1128/mcb.18.8.4471
53. Verrijdt G, Haelens A, Schoenmakers E, Rombauts W, Claessens F. Comparative analysis of the influence of the high-mobility group box 1 protein on DNA binding and transcriptional activation by the androgen, glucocorticoid, progesterone and mineralocorticoid receptors. *Biochem J*. 2002;361 (Pt 1):97–103. doi:10.1042/0264-6021:3610097